Kink Band Formation in Graphite under Ion Irradiation at 100 K and 298 K

Jonathan A. Hinks[1*], G. Greaves[1], Sarah J. Haigh[2], Cheng-Ta Pan[2] and Stephen E. Donnelly[1]

1. School of Computing and Engineering, University of Huddersfield, HD1 3DH, United Kingdom

2. School of Materials, University of Manchester, Material Science Centre, Grosvenor Street, Manchester, M13 9PL, United Kingdom

* Corresponding author, E-mail: j.a.hinks@hud.ac.uk

Abstract

The effects of displacing radiation in graphitic materials are important for technologies including nuclear power, graphitic-based nanocomposites and hybrid graphene-silicon high-speed integrated electronics. These applications expose graphitic materials to displacing irradiation either during manufacture and/or involve the deployment of these materials into irradiating environments. One of the most interesting phenomena in the response of graphite to irradiation is the formation of kink bands on the surface of the material. Here we apply the technique of transmission electron microscopy with *in situ* ion irradiation to observe the dynamic formation of these features. Kink bands were created at both 100 K and 298 K with doming of the samples also observed due to radiation induced dimensional change leading to mechanical deformation. Probably at 298 K, but certainly at 100 K, there should be no point defect mobility in graphite according to the latest theoretical calculations. However, some of the theories of dimensional change in graphite require point defect motion and agglomeration

in order to operate. The implications of the experimental results for existing theories and the possibility of thermal effects due to the ion irradiation are discussed.

Keywords: graphite; radiation damage; kink bands; ion irradiation

1. Introduction

Graphitic materials play a key role in many established and emergent technologies including hybrid graphene-silicon high-speed integrated electronics [1–3], graphene nanocomposite materials [1,4,5] and nuclear fission reactor designs both current (such as the advanced gas-cooled reactor [6]) and future (such as the Generation IV very high temperature and molten salt reactors [7]). The processing and deployment of these materials can expose them to displacing radiation which can cause significant modification to both their structure and properties [8].

Displacing radiation has been observed to create kink bands (sometimes characterised as twins) in graphite in a number of studies [9–13]. These ridge-like structures protrude from the surface of the material and can form extended networks which reflect the underlying crystallographic structure of the graphite. Here we report on the observation of the dynamic formation of these features at 100 K and 298 K. The latest theoretical calculations of migration energies give values of 1.0 eV [14] to 1.1 eV [15] for vacancies and 1.2 eV for interstitials [16]. Using a vibrational frequency of 5×10^{13} Hz [8], at 273 K these energies give maximum jump rates of only 6×10^{-4} Hz for vacancies and 2.5×10^{-7} Hz for interstitials. Therefore at room temperature, and certainly at 100 K, the interstitials and vacancies are not expected to be mobile. This raises the question as to the underlying atomistic mechanisms which drive the formation of these intriguing structures.

2. Experimental Procedure

Thin flakes of graphite were prepared using the micromechanical cleavage technique on highly orientated pyrolitic graphite (HOPG)]. The flakes were deposited onto an SiO_2 substrate and then optical microscopy was used to identify suitable specimens [17,18]. A layer of poly(methyl methacrylate) (PMMA) was spin-coated on top and then the substrate

was dissolved using KOH. Deionised water was used to wash the flakes which were then transferred to transmission electron microscopy (TEM) grids. Acetone was used to remove the PMMA layer leaving free-standing flakes of thin graphite. More details of the sample preparation procedures have been published previously [19,20].

TEM of graphite under *in situ* 30 keV Ar^+ or 60 keV Xe^+ ion irradiation was performed using the Microscope and Ion Accelerator for Materials Investigations (MIAMI) facility [21] at the University of Huddersfield, United Kingdom. The MIAMI facility is shown in Figure 1 and its specifications are summarised in Table 1. A low ion beam flux of 5×10^{10} ions.cm^{-2}.s^{-1} was used in order to minimise the effects of sample heating. The JEOL JEM-2000FX TEM at the MIAMI facility was operated at 80 kV to avoid the damaging effects of the electron beam known to occur at higher energies [22–24]. Images shown in the current paper were all captured in bright-field conditions with the sample tilted so as to avoid obfuscating strong diffraction-contrast wherever possible. The regions exposed to the electron beam during the experiments were compared to other ion irradiated areas to check for any significant contribution by the electron beam to the modification of the microstructure. The TEM samples were cooled to 100 K using a Gatan Model 636 double-tilt liquid-nitrogen cooled holder. Images and video were captured using a Gatan ORIUS SC200 digital camera. Video was captured at a frame size of 480×480 pixels and a video frame rate of 8 Hz.

3. Results and Discussions

3.1 Formation of Kink Bands

Kink bands were observed to form under 60 keV Xe^+ ion irradiation at both 100 K and 298 K as shown in Figures 2 and 3. At room temperature, the kink bands which formed in the area under observation did so in a sudden process which lasted less than one frame of video

(0.125 s) at a fluence of 1.4×10^{13} ions.cm^{-2}. However in the 100 K experiment, the kink bands were observed to form at the lower fluence of 5×10^{12} ions.cm^{-2} in a combination of continuous growth along their axis and sudden discreet events. At both temperatures, the kink bands were observed to widen in projection under continued irradiation. Finally, after ion irradiation was stopped the kink bands were found to be stable at room temperature as shown in Figures 2c and 3b. Comparison of areas followed during the irradiation (i.e. exposed to the electron beam) to other areas exposed to only the ion beam demonstrated no significant effect of the electron beam. Similarly, TEM observation of similar samples at higher electron beam energies up to 200 keV has not produced any of the features observed under 60 keV Xe^+ ion irradiation.

The cause of the formation and growth of the kink bands under displacing irradiation has been attributed to radiation-induced dimensional change in the graphite which varies as a function of depth due to the damage profile of the 60 keV Xe^+ ion irradiation [25]. This results in mechanical stress within the sample which then buckles creating the kink bands. The atomistic mechanisms behind the dimensional change are discussed below in section 3.2.

As shown in Figures 2a and 3a, the virgin samples contained a low density of broad bend contours indicating the graphite was relatively flat and unstrained. After kink band formation, the regions delineated by the bands featured significant levels of diffraction and moiré contrast as shown in Figures 2b, 2c and 3b. Moiré is frequently observed in TEM of graphitic samples viewed normal to the basal sheets as the planar structure allows misorientations to occur. The introduction of diffraction and moiré contrast demonstrates the strain which is present in the sample as a consequence of the ion irradiation. The formation of the kink bands – which are in effect a yielding and buckling of the material – is also evidence of considerable irradiation-induced stress.

3.2 Atomistic Origins of Radiation-Induced Stress

Traditional models of displacing radiation induced mechanical deformation in graphite involve the agglomeration of vacancies into loops within the basal sheets which then collapse [26,27]. The collapse of these loops induces strain not only in the host basal sheet but also in neighbouring sheets through interstitials which act as pinning sites between the sheets [28]. The latest theoretical calculations put the migration of energy of vacancies, E_m, at 1.0 eV [14] to 1.1 eV [15]. The vibrational frequency of the carbon atoms parallel to the basal sheets of graphite is about 5×10^{13} Hz [8]. Applying Boltzmann statistics to the migration of vacancies with this frequency as the prefactor gives jump rates as shown in Figure 4 for E_m = 1.0 eV. As can be seen, significant rates of vacancy migration are expected at temperatures above 350 K. Therefore, at the nominal irradiation temperatures of the experiments reported here (i.e. 100 K and 298 K) no vacancy migration would have occurred.

However, the possibility of ion beam heating of the sample must be considered. At the low ion flux used in these experiments (5×10^{10} ions.cm^{-2}.s^{-1}), a typical atomic collision cascade as calculated using SRIM [29] would affect a given area on average approximately every 20 s. In the sample geometry used, there is large contact surface area between the graphite flakes and the TEM grids. Therefore the heat would have had plenty of time to dissipate and the TEM grid would have acted as an efficient heat sink. On the basis of these considerations, it is unlikely that any significant ion beam induced heating of the samples could have occurred. It is certainly the case that the sample in the nominally 100 K irradiation could not have been heated to the temperatures required to activate vacancy migration.

Another possibility is that vacancies are able to agglomerate during the thermal phase following each atomic collision cascade. The thermal phase lasts on the order of

10 ps which is equivalent to around 500 atomic vibrations. During this brief period, the temperature within the cascade volume is elevated but rapidly decays. Molecular dynamic simulations of atomic collision cascades typically predict that 20% of point defects survive the ballistic and thermal phases – i.e. do not undergo recombination [30,31]. In order for vacancies to agglomerate within these very short timescales, the remaining defects must be highly mobile and it remains unclear if sufficient rates of migration could be achieved. Further work is underway to explore whether any significant effects can occur during the thermal phase and the atomistic processes involved.

As mechanical deformation is observed at temperatures below that at which vacancy migration can occur and if ion-beam heating effects are excluded, other possibilities must be considered. For example, a model based on the rucking of the basal sheets driven by the agglomeration of basal dislocations has been proposed [28]. Such a mechanism could operate at lower temperatures due to the low energy barrier to basal dislocation glide. Another intriguing possibility is offered by the deformation of graphene due to structural defects which lead to out-of-plane buckling [32,33]. By relaxing into the third dimension, a two-dimensional sheet can exchange in-plane elastic energy for bending energy. Calculations using Molecular dynamics [34,35], *ab initio* [36] and continuum theory [37] have predicted that such behaviour can occur at dislocations and grain boundaries. Furthermore, there is experimental evidence for buckling of graphene from atomic force microscopy [38], scanning tunnelling microscopy [39] and high resolution TEM [40]. However, to date such phenomena have been reported in work on graphene and it is uncertain if they could occur with graphite.

3.3 Temperature and Fluence Dependence

Repeat experiments in the current study have shown that the fluence for kink band formation in different samples can vary when irradiated under the same temperature and ion beam conditions. This suggests that there are variables other than the irradiation conditions which determine the threshold fluence – for example sample thickness, pre-existing defects, local constraints applied by support grid etc. Therefore it is not possible to draw conclusions regarding the threshold fluence for kink band formation as a function of temperature. Further work is underway to explore the effect temperature has on threshold fluence and kink band network morphology.

3.4 Formation of Bend Contour Patterns

Under appropriate diffraction conditions, bend contour networks such as that shown in Figure 5a can be observed after kink band formation. These occur where the strain between the kink bands causes the sample to bulge outwards from the basal plane forming a domed region. At the point on the surface of the dome at which the [0001] down-zone condition is satisfied, a zone axis pattern is observed formed by the intersection of bend contours corresponding to the {1 1 0 0 } reflections. Each kink-band-bounded area in an appropriately orientated and strained sample can be observed to be decorated in this way and collectively these form a network of bend contour patterns. Figure 5b shows a schematic visualisation of how the surface of the sample is expected to be domed in the regions surrounded by the kink bands.

4. Conclusion

Thin single crystals of graphite have been 60 keV Xe ion irradiated *in situ* within a TEM at 100 K and 298 K. Under these conditions, networks of kink bands have been observed to form due to the radiation-induced stresses within the samples. At room temperature, the

energy of vacancy migration energy may allow the point defect model of mechanical deformation in graphite to operate. However, at 100 K the mobility of vacancies is too low for this to occur at the nominal irradiation temperature. This leads to consideration of the possibility that phenomena occur within the collision cascade and subsequent thermal phase following each ion impact. However, other theories exist in the literature which do not require point defect mobility and these also offer alternative explanations. Finally, strain in the regions bounded by the kink bands has been found to form networks of bend contour patterns due to local doming of the sample.

Acknowledgments

The authors would like to thank the Engineering and Physical Sciences Research Council (United Kingdom) for funding under grant numbers EP/I003223/1 and EP/G035954/1; and the Defence Threat Reduction Agency (USA) for funding under grant number HDTRA-1-12-0013.

References

[1] K.S. Novoselov, V.I. Fal'ko, L. Colombo, P.R. Gellert, M.G. Schwab, K. Kim, Nature 490 (2012) 192.

[2] T. Georgiou, R. Jalil, B.D. Belle, L. Britnell, R. V Gorbachev, S. V Morozov, Y.-J. Kim, A. Gholinia, S.J. Haigh, O. Makarovsky, L. Eaves, L.A. Ponomarenko, A.K. Geim, K.S. Novoselov, A. Mishchenko, Nat. Nanotechnol. 8 (2013) 100.

[3] S.J. Haigh, A. Gholinia, R. Jalil, S. Romani, L. Britnell, D.C. Elias, K.S. Novoselov, L.A. Ponomarenko, A.K. Geim, R. Gorbachev, Nat. Mater. 11 (2012) 764.

[4] R.J. Young, I.A. Kinloch, L. Gong, K.S. Novoselov, Compos. Sci. Technol. 72 (2012) 1459.

[5] L. Gong, R.J. Young, I.A. Kinloch, I. Riaz, R. Jalil, K.S. Novoselov, ACS Nano 6 (2012) 2086.

[6] B.J. Marsden, G.N. Hall, Comp. Nucl. Mater. 4 (2012) 325.

[7] Y. Guérin, G.S. Was, S.J. Zinkle, G. Editors, Mater. Res. Soc. Bull. 34 (2009) 10.

[8] B.T. Kelly, Physics of Graphite, Applied Science Publishers, Barking, England, 1981.

[9] K. Niwase, T. Tanabe, M. Sugimoto, F.E. Fujita, J. Nucl. Mater. 162-164 (1989) 856.

[10] T. Tanabe, Phys. Scr. T64 (1996) 7.

[11] D.J. Bacon, I. Dumler, A.S. Rao, J. Nucl. Mater. 103-104 (1981) 427.

[12] D.J. Bacon, A.S. Rao, J. Nucl. Mater. 91 (1980) 178.

[13] E.J. Freise, A. Kelly, Proc. R. Soc. A 264 (1961) 269.

[14] G.-D. Lee, C. Wang, E. Yoon, N.-M. Hwang, D.-Y. Kim, K. Ho, Phys. Rev. Lett. 95 (2005) 205501.

[15] C.D. Latham, M.I. Heggie, M. Alatalo, S. Oberg, P.R. Briddon, J. Phys. Condens. Matter 25 (2013) 135403.

[16] Y. Ma, Phys. Rev. B 76 (2007) 075419.

[17] P. Blake, E.W. Hill, A.H. Castro Neto, K.S. Novoselov, D. Jiang, R. Yang, T.J. Booth, A.K. Geim, Appl. Phys. Lett. 91 (2007) 063124.

[18] Z.H. Ni, H.M. Wang, J. Kasim, H.M. Fan, T. Yu, Y.H. Wu, Y.P. Feng, Z.X. Shen, Nano Lett 7 (2007) 2758.

[19] K.S. Novoselov, A.K. Geim, S. V Morozov, D. Jiang, Y. Zhang, S. V Dubonos, I. V Grigorieva, A.A. Firsov, Science (80-.). 306 (2004) 666.

[20] J.C. Meyer, C.O. Girit, M.F. Crommie, A. Zettl, Nature 454 (2008) 319.

[21] J.A. Hinks, J.A. van den Berg, S.E. Donnelly, J. Vac. Sci. Technol. A 29 (2011) 021003.

[22] C. Karthik, J. Kane, D.P. Butt, W.E. Windes, R. Ubic, J. Nucl. Mater. 412 (2011) 321.

[23] D.F. Pedraza, J. Koike, Carbon N. Y. 32 (1994) 727.

[24] J. Koike, D. Pedraza, Mater. Res. Soc. Proc. 279 (1992) 67.

[25] J.A. Hinks, S.J. Haigh, G. Greaves, F. Sweeney, C.T. Pan, R.J. Young, S.E. Donnelly, Carbon N. Y. (2013).

[26] T.D. Burchell, L.L. Snead, J. Nucl. Mater. 371 (2007) 18.

[27] R.H. Telling, M.I. Heggie, Phil. Mag. 87 (2007) 4797.

[28] M.I. Heggie, I. Suarez-Martinez, C. Davidson, G. Haffenden, J. Nucl. Mater. 413 (2011) 150.

[29] J.F. Ziegler, M.D. Ziegler, J.P. Biersack, Nucl. Instrum. Meth. B 268 (2010) 1818.

[30] K. Nordlund, M. Ghaly, R. Averback, M. Caturla, T. Diaz de la Rubia, J. Tarus, Phys. Rev. B 57 (1998) 7556.

[31] V.A. Borodin, Nucl. Instrum. Meth. B 282 (2012) 33.

[32] F. Banhart, J. Kotakoski, A. V Krasheninnikov, ACS Nano 5 (2011) 26.

[33] F. Cataldo, Carbon N. Y. 40 (2002) 157.

[34] Y. Liu, B.I. Yakobson, Nano Lett. 10 (2010) 2178.

[35] T.-H. Liu, G. Gajewski, C.-W. Pao, C.-C. Chang, Carbon N. Y. 49 (2011) 2306.

[36] O. V. Yazyev, S.G. Louie, Phys. Rev. B 81 (2010) 195420.

[37] S. Chen, D.C. Chrzan, Phys. Rev. B 84 (2011) 214103.

[38] H.C. Schniepp, K.N. Kudin, J.-L. Li, R.K. Prud'homme, R. Car, D. a Saville, I. a Aksay, ACS Nano 2 (2008) 2577.

[39] J. Coraux, A.T. N'Diaye, C. Busse, T. Michely, Nano Lett 8 (2008) 565.

[40] A. Hashimoto, K. Suenaga, A. Gloter, K. Urita, Nature 430 (2004) 17.

List of Captions of Tables and Figures

Figure 1: The Microscope and Ion Accelerator for Materials Investigations (MIAMI) facility at the University of Huddersfield, United Kingdom: (a) computer-generated model showing the layout of the ion beam system and the interfacing with the TEM; and (b) a photograph of the facility showing the bending magnet (top left) and the JEOL JEM-2000FX TEM (right).

Figure 2: Bright field TEM micrographs of kink bands formed in graphite under in situ 60 keV Xe^{+} ion irradiation at 100 K: (a) virgin sample; (b) after 1.8×10^{13} ions.cm^{-2}; and (c) after heating to room temperature. The scale marker in the first panel applies to all three micrographs.

Figure 3: Bright field TEM micrographs of kink bands formed in graphite under in situ 60 keV Xe^{+} ion irradiation at 298 K: (a) virgin sample; and (b) after 1.8×10^{13} ions.cm^{-2}. The scale marker in the first panel applies to both micrographs.

Figure 4: Graph showing vacancy jump rates in graphite as a function of temperature assuming an activation energy E_m = 1.0 eV and an in-plane vibrational frequency of 5×10^{13} Hz [8].

Figure 5: Bend contour network observed in ion irradiated graphite: (a) TEM micrograph; (b) schematic visualisation with cutaway section through sample (dimensions of the kink bands have been enhanced for clarity). Each bend contour pattern resides in a region bounded by kink bands formed in response to the irradiation-

induced stress in the sample. These regions are domed with the centre of the associated bend contour pattern indicating the location of the [0001] down-zone condition.

Table 1: Overview of the specifications of the MAIMI facility

Figure 1

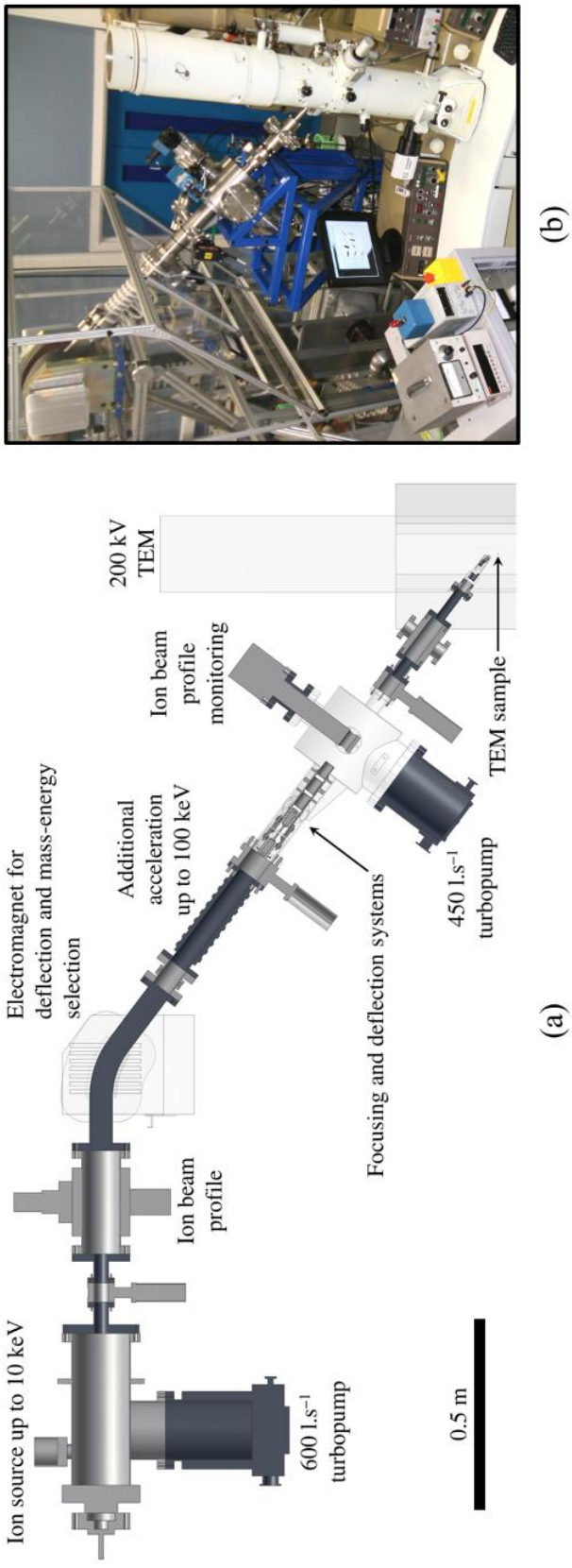
(b)
200 kV
TEM
Ion beam
profile
monitoring
Electromagnet for
deflection and mass-energy
selection
Additional
acceleration
up to 100 keV
Ion beam
profile
Focusing and deflection systems
450 l.s⁻¹
turbopump
TEM sample
Ion source up to 10 keV
600 l.s⁻¹
turbopump
0.5 m
(a)

Figure 2

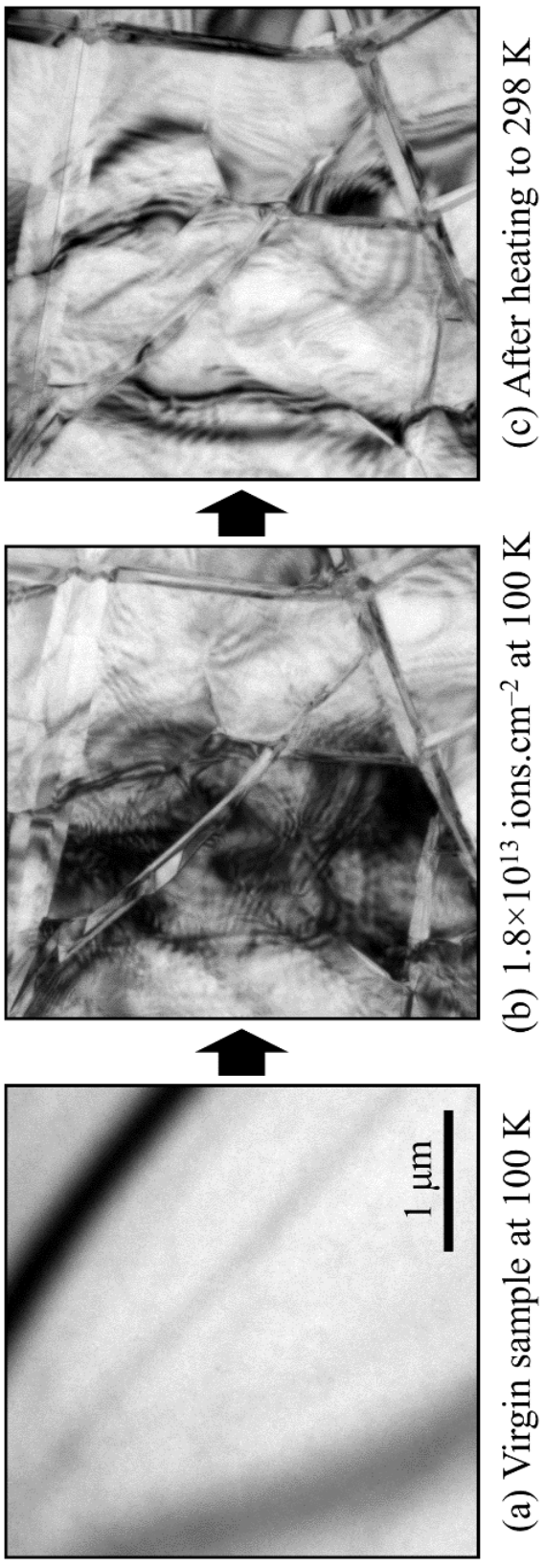
1 μm
(a) Virgin sample at 100 K
(b) 1.8×10¹³ ions.cm⁻² at 100 K
(c) After heating to 298 K

Figure 3

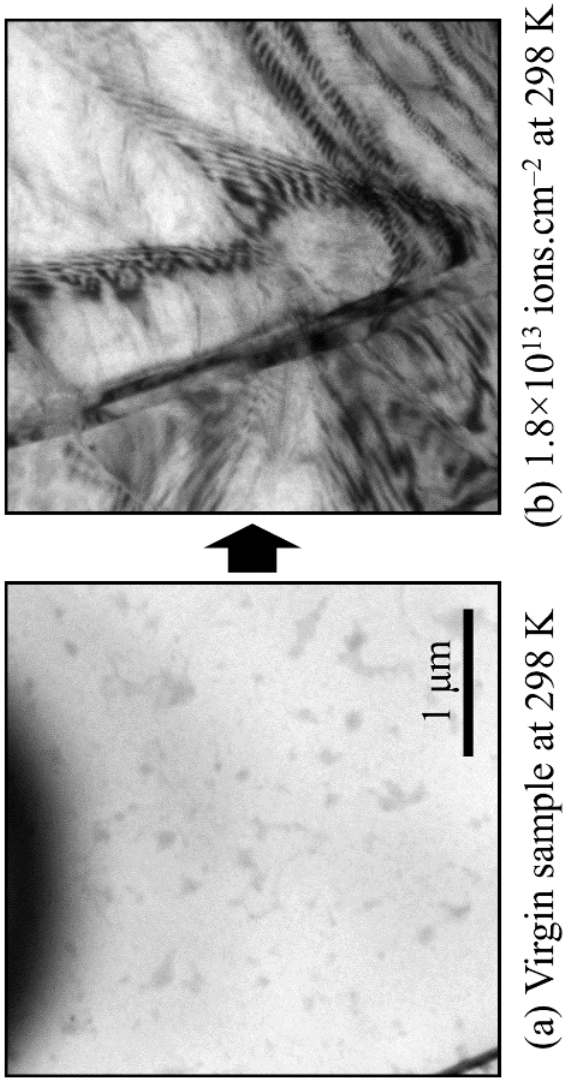

Figure 4

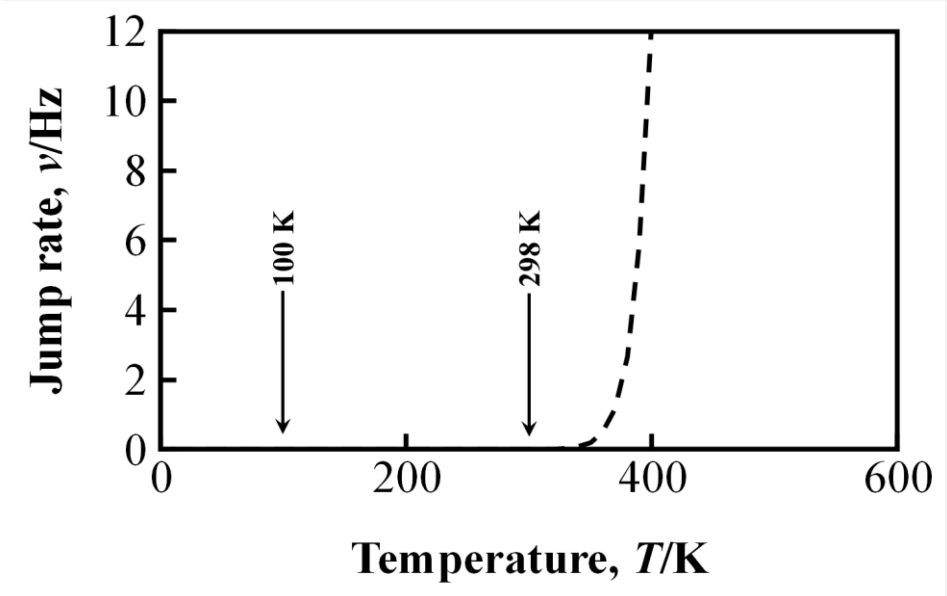
Jump rate, ν/Hz
12
10
8
6
4
2
0
100 K
298 K
0
200
400
600
Temperature, T/K

Figure 5

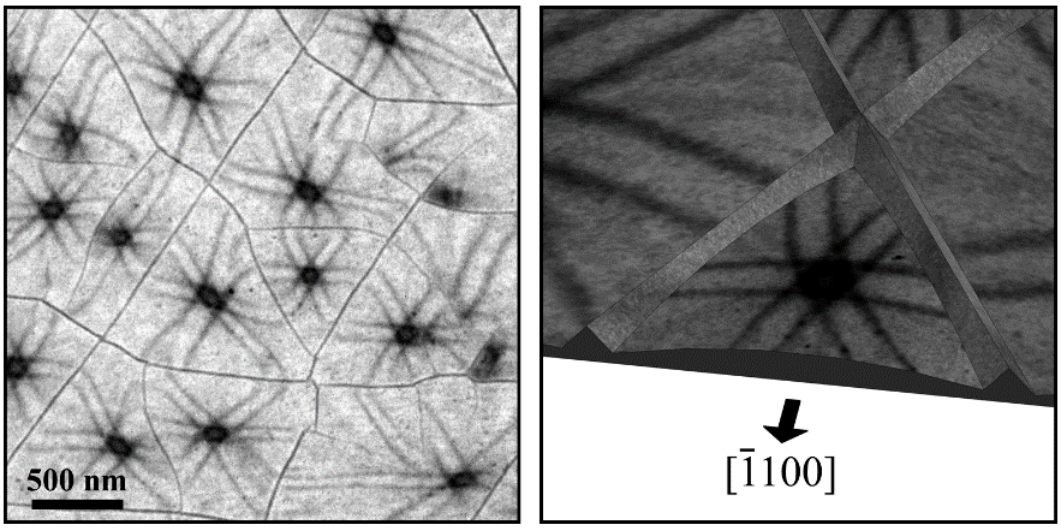

(a) (b)

Table 1

Microscope and Ion Accelerator for Materials Investigations (MIAMI)

Transmission electron microscope	JEOL JEM-2000FX
Electron beam accelerating voltage	80 to 200 kV
Ion beam accelerating voltage	1 to 100 kV
Ionic species available	Most elements from He to Xe
Typical ion flux	2×10^{13} $cm^{-2}.s^{-1}$ for 10 keV He
Angle between electron and ion beams	30° (previously 25°)
Sample temperature	100 to 380 K or RT to 1270 K
Image capture	Gatan ORIUS SC200 (4 megapixels)